Discovery of Boronic Acids-Based β-Lactamase Inhibitors Through In Situ Click Chemistry

Nicolò Santi , Alessandra Piccirilli , Mariagrazia Perilli , Robert A. Bonomo , Francesco Fini , Fabio Prati , Emilia Caselli *

Posted Date: 7 March 2025

doi: 10.20944/preprints202503.0489.v1

Keywords: *in situ* click chemistry; boronic acid; beta-lactamase inhibitors; KTGS; antimicrobial resistance; BATSI

 doi:10.20944/preprints202503.0489.v1

Article

Discovery of Boronic Acids-Based β-Lactamase Inhibitors Through In Situ Click Chemistry

Nicolò Santi [1], Alessandra Piccirilli [2], Mariagrazia Perilli [2], Robert A. Bonomo [3], Francesco Fini [1], Fabio Prati [1] and Emilia Caselli [1,*]

[1] Department of Life Sciences, Università degli studi di Modena e Reggio Emilia (UNIMORE), via Campi 103, 41125 Modena, Italy

[2] Department of Biotechnological and Applied Clinical Sciences, University of L'Aquila, via Vetoio, 67100 L'Aquila, Italy

[3] Case Western Reserve University, School of Medicine, Cleveland, OH, USA; Research Service, Louis Stokes Cleveland Department of Veterans Affairs Medical Center, Cleveland, OH, USA; Clinician Scientist Investigator, Louis Stokes Cleveland Department of Veterans Affairs Medical Center, Cleveland, OH, USA; Departments of Medicine, Pharmacology, Molecular Biology and Microbiology, Biochemistry, and Proteomics and Bioinformatics, Case Western Reserve University School of Medicine, Cleveland, OH, USA; CWRU-Cleveland VAMC Center for Antimicrobial Resistance and Epidemiology (Case VA CARES), Cleveland, OH, USA

* Correspondence: emilia.caselli@unimore.it; Tel.: +39 059 205 8586

Abstract: In this study we evaluated *in situ* click chemistry as platform for discovering boronic acid-based β-lactamase inhibitors (BLIs). Unlike conventional drug discovery approaches requiring multi-step synthesis, protection strategies, and extensive screening, the *in situ* method can allow the generation and identification of potent β-lactamase inhibitors in a rapid, economic and efficient way. Using KPC-2 (class A carbapenemase) and AmpC (class C cephalosporinase) as templates, we demonstrated their ability to catalyse azide-alkyne cycloaddition, facilitating the formation of triazole-based β-lactamase inhibitors. Initial screening of various β-lactamases and boronic warheads identified compound **3** (3-azidomethylphenyl boronic acid) as the most effective scaffold for Kinetic Target-Guided Synthesis (KTGS). KTGS experiments with AmpC and KPC-2 yielded triazole inhibitors with K_i values as low as 140 nM (compound **10a**, AmpC) and 730 nM (compound **5**, KPC-2). Competitive inhibition studies confirmed triazole formation within the active site, while LC-MS analysis verified that the reversible covalent interaction of boronic acids did not affect detection of the *in situ* synthesised product. While KTGS successfully identified potent inhibitors, limitations in amplification coefficients and spatial constraints highlight the need for optimised warhead designs. This study validates KTGS as a promising strategy for BLI discovery and provides insights for further refinement in fighting β-lactamase-mediated antibiotic resistance.

Keywords: *in situ* click chemistry; boronic acid; beta-lactamase inhibitors; KTGS; antimicrobial resistance; BATSI

1. Introduction

Nearly a century after penicillin's discovery, the development of new antibiotics continues to lag behind the rapid evolution of antimicrobial resistance (AMR), which has significantly impacted β-lactams, the most widely used bactericidal agents.[1,2] Among various resistance mechanisms in Gram-negative bacteria, β-lactamase expression plays a dominant role by hydrolysing the β-lactam ring, rendering these antibiotics ineffective.[3–6] β-Lactamases are classified into serine β-lactamases (SBLs; classes A, C, D) and metallo-β-lactamases (MBLs; class B), each with distinct hydrolytic mechanisms. [7–10] Contemporary and highly clinically relevant enzymes, such as KPCs, NDMs, and OXAs families, contribute to resistance against expanded-spectrum cephalosporins (ceftazidime,

 doi:10.20944/preprints202503.0489.v1

ceftolozane and cefidericol), monobactams, and even carbapenems, threatening the efficacy of "last-resort" antibiotics.[11–15]

Boronic acid transition state inhibitors (BATSIs) are covalent, reversible inhibitors mimicking the high-energy tetrahedral intermediate during β-lactam hydrolysis, offering a promising strategy against both SBLs and MBLs (Figure 1). [16–18] The success of cyclic BATSIs, including commercially available Vaborbactam and Phase III and I candidates Taniborbactam and Xeruborbactam, highlights their clinical relevance.[4,19–28] During the past decades, our group has developed a vast library of acyclic BATSIs.[17,29–34] Incorporation of a triazole group in β-position of the boron atom led to the generation of potent BATSIs, including **MB076** and **S02030**, both exhibiting strong activity against class A and C β-lactamases.[17,19,35,36]

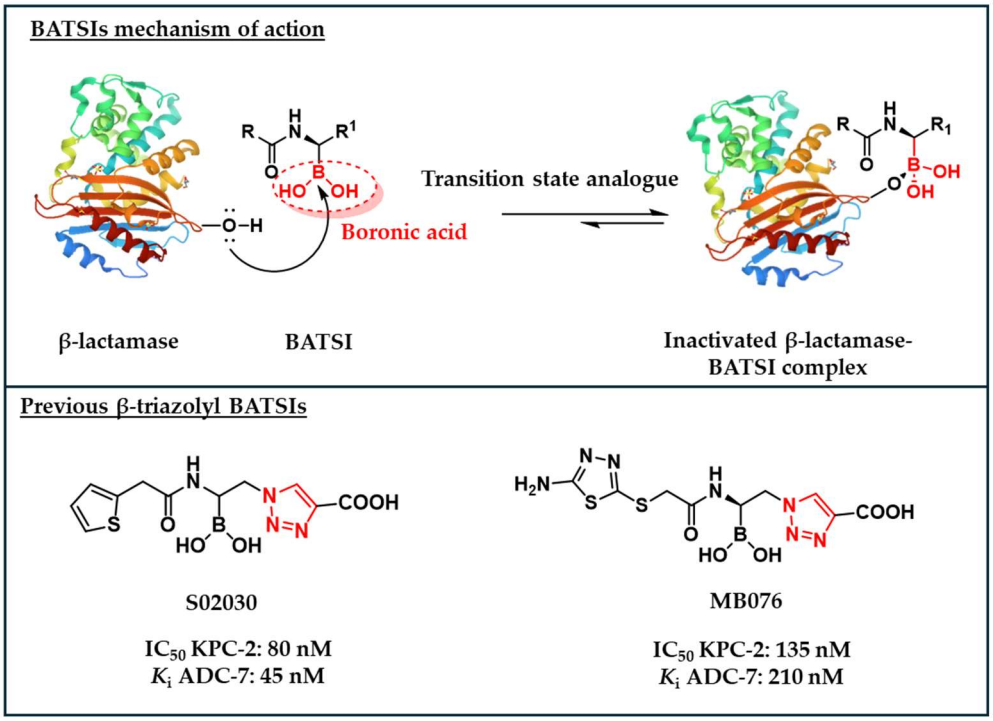

Figure 1. Top panel: BATSIs mechanism of action against β-lactamases. Bottom panel: structures and biochemical parameters of β-lactamase inhibition of **S02030** and **MB076**.

Both **S02030** and **MB076** feature a 1,4-disubstituted 1,2,3-triazole moiety, synthesised via Copper-catalysed Azide-Alkyne Cycloaddition (CuAAC).[17] The triazole's affinity for the β-lactamases active site, combined with the broad availability of azides and alkynes, opens up opportunities for creating novel BATSIs.[37,38]

In this context, an attractive approach to obtain triazole-decorated molecules is represented by Kinetic Target-Guided Synthesis (KTGS), an appealing drug discovery method where the target protein catalyses the synthesis of its own inhibitors.[39] In KTGS the protein-templated synthesis of bioactive compounds is achieved once the target facilitates the approaching of affine reagents with proper orientation, therefore lowering the energy of activation required for their irreversible binding.[39] KTGS allows efficient screening of small molecules, particularly through *in situ* click chemistry, where the target enzyme guides the formation of disubstituted 1,2,3-triazoles from azides and alkynes.[40–48] *In situ* click chemistry efficiency is driven by the ability of the target enzyme to overcome the high energy of activation required for (3+2) cycloaddition reactions (>25–30 kcal/mol).[49–51] Successful examples of this technique are mostly focused on the generation of non-covalent compounds, starting from previously reported inhibitors in a binary format (pairs of reagents).[39] Although KTGS has been known for more than two decades, reports on its application remain relatively infrequent, with only a few unsuccessful examples documented in the literature.[39,52,53] With fewer than 10% of KTGS studies focusing on covalent inhibitors, examples

 doi:10.20944/preprints202503.0489.v1

of this approach have not yet been reported for developing BATSIs or BLIs.[39,46] This highlights an untapped potential in using KTGS for covalent drug discovery, specifically in the design of novel inhibitors targeting β-lactamases.

Among the various KTGS formats available, the multicomponent format (involving a cluster of reagents) enables broader exploration compared to the binary format (pairing two reagents), facilitating faster and more efficient screening.[39] To accelerate BATSIs development and expand the KTGS scope, we applied a multicomponent *in situ* click chemistry approach using KPC-2 (class A) and chromosomal AmpC (class C) β-lactamases as templates (Figure 2). Our strategy involves synthesising azido-functionalised boronic acid "warheads", leveraging the ability of boron to selectively target the β-lactamase catalytic serine located in the active site. The azido group enables further exploration within the active site through reactions with various alkynes, forming potentially bioactive triazoles. This work represents the first attempt to perform *in situ* click chemistry to develop triazole-based BATSIs using β-lactamases as scaffolds and a 90-component alkyne library to explore new chemical space.

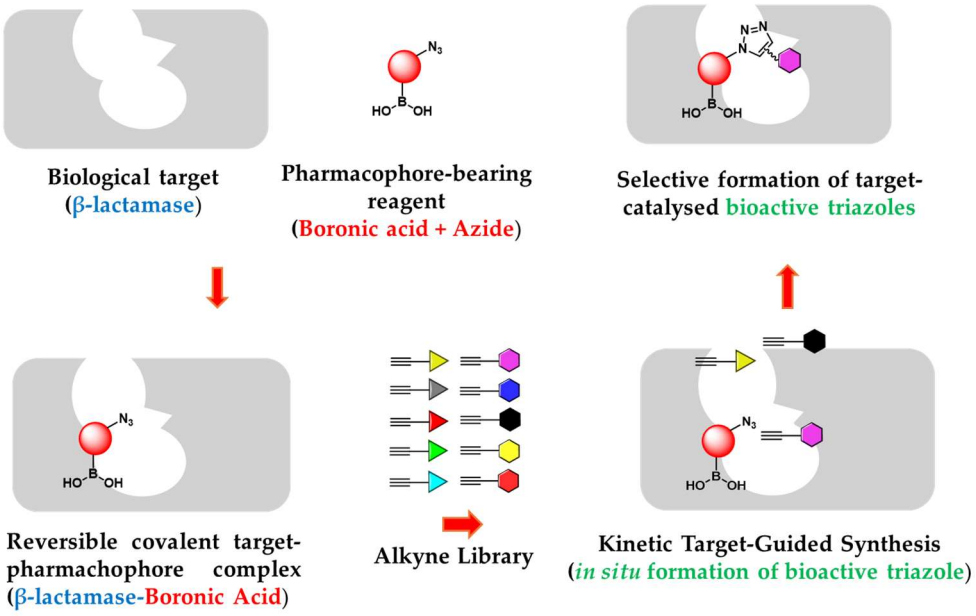

Figure 2. Aim of the work.

2. Results

2.1. Design and Synthesis of the Warhead

KTGS allows the development of potent inhibitors without prior knowledge of their target affinities, provided that one of the two components demonstrates sufficient affinity to act as an anchor molecule.[50] Previously, even a low level of affinity was reported to be sufficient for the target-templated reaction.[50] Therefore, to enable *in situ* click chemistry within the β-lactamase's binding pocket, a series of bifunctional "warheads" displaying two defined features were designed. Firstly, the presence of the boronic acid moiety serves as anchor to the SBLs catalytic serine. Secondly, the azido functionalisation guarantees the clickable building block for generation of bioactive triazoles within the target active site. Thus, one 2-azido-1-acylamino-ethaneboronic acid and three azidomethyl-phenylboronic acids were synthesised and characterised (Figure 3). Inspired by one of the most potent BATSI, **S02030** (Figure 2),[17,19,36] compound **1** was obtained through deprotection of the corresponding pinanediol ester, following a previously reported procedure.[17] Herein, the amide side chain from cephalothin is well-known to interact with various β-lactamases through Van der Waals and H-bonding interactions and can aid the process of recognition within the target.[54] Although, being a promising scaffold for potential novel inhibitors, we observed by ^{1}H NMR studies

 doi:10.20944/preprints202503.0489.v1

that compound **1** partially degrades in phosphate buffer (see supplementary information, figures S1 and S2); therefore, this warhead was excluded from further studies.

Phenyl boronic acids bearing 1,4-disubstituted 1,2,3-triazoles at the *m*- and *p*- positions were reported as potent inhibitors of KPC-2 by Zhou *et al.*[55,56] Interestingly, the azido starting materials, (3-(azidomethyl)phenyl)boronic acid (**3**) and (4-(azidomethyl)phenyl)boronic acid (**4**), were reported exhibiting sub μM activity vs KPC-2.[56] Inspired by those scaffolds, compound **2** was also included. Whereas the role of phenyl boronic acids as BLIs have been extensively discussed in the past decades, KTGS might allow further refining for this class of inhibitors. Chemically, azido derivatives **2**, **3** and **4** were synthesised via a single step transformation starting from the respective bromo-derivatives, following previously reported procedures.[55,56]

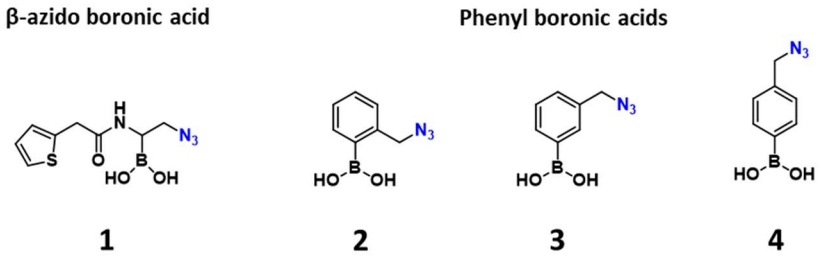

Figure 3. Structure for the designed warheads.

2.2. Inhibition (%) of the Warheads on Representative BLs

Selection of an appropriate warhead-bearing reagent is crucial for achieving a successful *in situ* click chemistry.[39] Thus, we assessed the inhibitory activity of the selected warheads against a pool of different β-lactamases to verify their binding specificity for the target. The affinity (inhibitory ability) of **2-4** against 12 representative β-lactamase from class A, B, C and D was assessed as percentage of inhibition at a fixed concentration of 200 μM (Table 1). For both KPC-2 and chromosomal AmpC, this percentage was lowered to 100 μM due to high activity of some of the warheads at 200 μM.

Table 1. % of inhibition at a fixed concentration of 200 μM for warheads **1-4** against 12 β-lactamases.

Entry	β-lactamase[1]	Class	**2**	**3**	**4**
1	KPC-2[2]	A	35	**76**	72
2	CTX-M-15		0	42	22
3	KPC-53		54	65	55
4	SHV-12		14	38	48
5	NDM-1	B	23	20	24
6	VIM-1		23	24	33
7	IMP-1		12	11	22
8	AmpC[2]	C	57	**100**	81
9	ADC-25		27	67	46
10	CMY-2		19	79	67
11	OXA-24	D	20	24	26
12	OXA-48		<1	2	<1

[1] Substrates, proteins and substrates concentrations, and relative constants are reported in section 4.3. [2] % of inhibition at 100 μM.

Unsurprisingly, phenylboronic acids displayed better activity against class A and C, while they are less prone to inhibition vs MBLs and class D. Among compounds **2-4,** the *m*-derivative **3** exhibited the best activity at 100 μM for KPC-2 and chromosomal AmpC, with 76% (Entry 1) and 100% (Entry

 doi:10.20944/preprints202503.0489.v1

8) of inhibition respectively. Thus, cpd **3** was chosen as ideal warhead-bearing reagent and AmpC and KPC-2 as target proteins to start the *in situ* click chemistry screening.

2.3. Generation of a 90-Component Alkyne Library

To facilitate KTGS in a multicomponent format with the azido-bearing warhead **3**, a diverse 90-member alkyne library was designed (Figure 4).[45,57] Based on their availability, alkynes were either purchased from commercial sources or synthesised through a 1- or 2- step synthesis. Synthesis was carried out mostly using propargyl amine, propargyl alcohol or propargyl bromide as sources of the alkyne functional group (see SI). To explore chemical diversity on the potential bioactive triazoles formed, the library was divided in 10 clusters containing 9 alkynes each. Clusters were created by including alkynes capable of interacting with the target via van der Waals force (columns 1 and 2), π-stacking and H-bonding (columns 3, 6, 7, and 8), π-cation, π-anion and H-bonding (columns 4 and 5). A miscellany of different relevant alkynes capable of interacting with the β-lactamases active site through some of the above interactions were included in the last two columns.

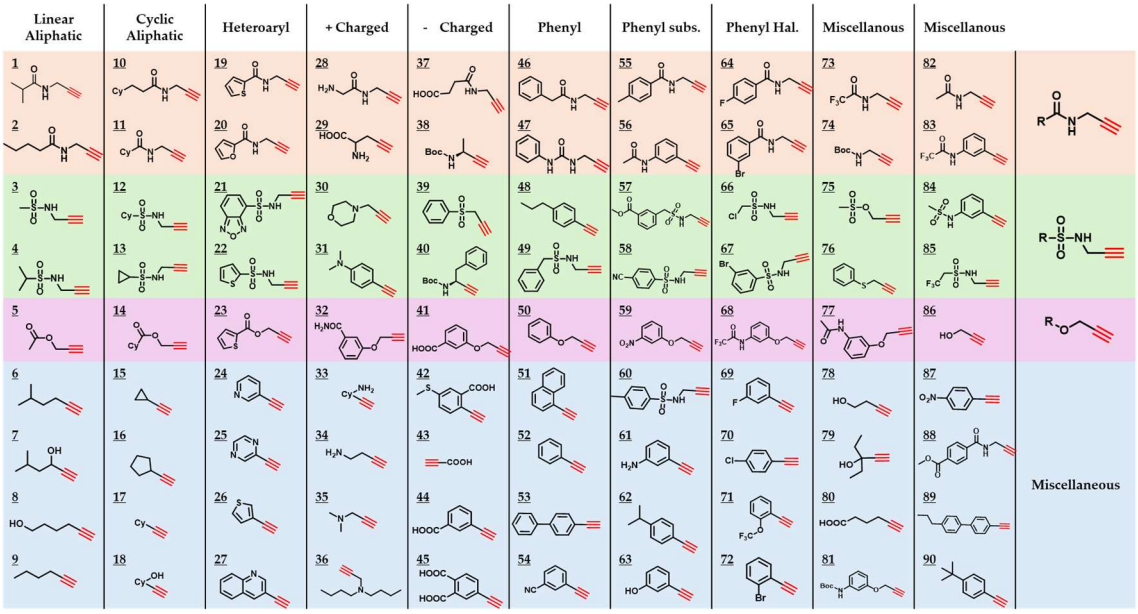

Figure 4. 90-component alkyne library. Alkynes are separated in 10 clusters (columns) by their chemical and steric properties. In each cluster are contained 9 alkynes, generally including an amido group (orange rows), sulfonamides (green rows) and ester or ether (magenta rows) scaffold.

2.4. In Situ Click Chemistry with KPC-2

Based upon the outcome of Table 1, initial efforts to perform the multicomponent *in situ* click chemistry were attempted using KPC-2 as template. Starting from the azido-functionalised boronic acid **3** optimised conditions (see SI Table S2) were applied in combination with the 90-component alkyne library. The reactions were conducted in 0.2 mL microtubes, in a mixture 95:5 sodium phosphate 50 mM pH 7.0:DMSO (final volume 100 μL) stirring at 300 rpm at 37 °C for 24 h (Scheme 1).

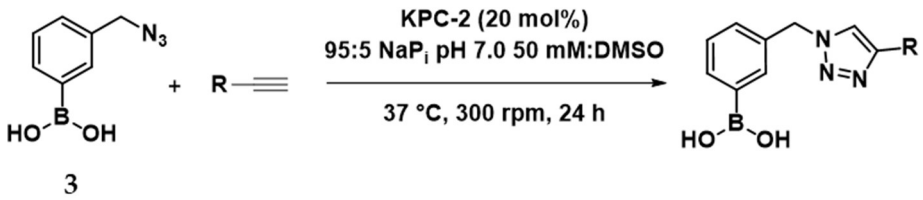

Scheme 1. Multicomponent *in situ* click chemistry between **3** and an alkyne library in presence of KPC-2.

 doi:10.20944/preprints202503.0489.v1

The experiments were conducted in triplicate, using a reaction mixture containing 1 equivalent of warhead **3**, 5 equivalents of each alkyne cluster (9 alkynes), and 20 mol% KPC-2 as the catalyst. Product formation was monitored directly from the crude mixture using a hybrid quadrupole orbitrap LC-MS system in ESI+ or ESI- mode after 24 h. Peak areas of the desired products were compared across three conditions: with KPC-2, without any enzyme, and with bovine serum albumin (BSA). Both no enzyme and BSA were used as controls, therefore only a negligible amount of product was expected to be observed in their presence. The resulting ratio, named as amplification coefficient (AC), was calculated from the peak area of the product obtained in presence of KPC-2 vs the one acquired with the controls.[58,59] CuAAC reactions employing $CuSO_4$, sodium ascorbate, and Tris(3-hydroxypropyltriazolylmethyl)amine (THPTA) served as control, regioselectively yielding the 1,4-regioisomer. To evaluate the presence of the 1,5-regioisomer in the KTGS experiment, a second control was obtained using thermal reaction conditions (80 °C for 24 hours), which resulted in a mixture of both 1,4- and 1,5-regioisomers. Out of 90 potential combinations, three triazole-based BATSIs (triazoles deriving from alkynes **Al-32**, **Al-39**, and **Al-57**) were identified with AC values exceeding 3, compared to the controls (Figure 5). Whereas the derivative from **Al-39** was exclusively formed as 1,4-regioisomer in presence of KPC-2, both derivates from **Al-32** and **Al-57** were observed as mixture of regioisomers. Interestingly, previously reported KPC-2 inhibitor 1,4-disubstituted 1,2,3-triazoles were not detected in this experiment, despite their known inhibition constants (K_i) for KPC-2, ranging from 32 nM to 1 μM (alkyne derivative = cyclopropyl (**Al-15**), 3-pyridinyl (**Al-24**), 3-thiophenyl (**Al-26**), COOH (**Al-43**), and phenyl substituents (**Al-52**)).[55,56]

Amplification coefficient vs negative controls (No protein and BSA)									
N.F.			0 > AC > 1		1 > AC > 3		AC > 3		
Cluster 1	Cluster 2	Cluster 3	Cluster 4	Cluster 5	Cluster 6	Cluster 7	Cluster 8	Cluster 9	Cluster 10
Al-1	Al-10	Al-19	Al-28	Al-37	Al-46	Al-55	Al-64	Al-73	Al-82
Al-2	Al-11	Al-20	Al-29	Al-38	Al-47	Al-56	Al-65	Al-74	Al-83
Al-3	Al-12	Al-21	Al-30	Al-39	Al-48	Al-57	Al-66	Al-75	Al-84
Al-4	Al-13	Al-22	Al-31	Al-40	Al-49	Al-58	Al-67	Al-76	Al-85
Al-5	Al-14	Al-23	Al-32	Al-41	Al-50	Al-59	Al-68	Al-77	Al-86
Al-6	Al-15	Al-24	Al-33	Al-42	Al-51	Al-60	Al-69	Al-78	Al-87
Al-7	Al-16	Al-25	Al-34	Al-43	Al-52	Al-61	Al-70	Al-79	Al-88
Al-8	Al-17	Al-26	Al-35	Al-44	Al-53	Al-62	Al-71	Al-80	Al-89
Al-9	Al-18	Al-27	Al-36	Al-45	Al-54	Al-63	Al-72	Al-81	Al-90

Figure 5. Cold map for the *in situ* click chemistry screening using KPC-2. Each cell corresponds to an alkyne. In dark blue are denoted alkynes that generated triazoles with AC > 3 in presence of the protein template.

To verify their biological activity, compounds **5** (triazole derivative from **Al-32**), **6** (derivative from **Al-39**), and **7** (derivative from **Al-57**) were synthesised, purified, and characterised at bench scale (Figure 6). Some control compounds, which either were not formed in the KTGS experiment or had AC values below 3 during the KPC-2 screenings, were also synthesised for comparative analysis; thus, derivatives **8** (from **Al-2**), **9** (Al-7), **10** (**Al-12**) and **11** (**Al-31**) were also prepared. Given KPC-2 did not dictate the majoritarian formation of the 1,5-regioisomer in any of the selected compounds, **5**-**11** were synthesised only as 1,4-regioisomers.

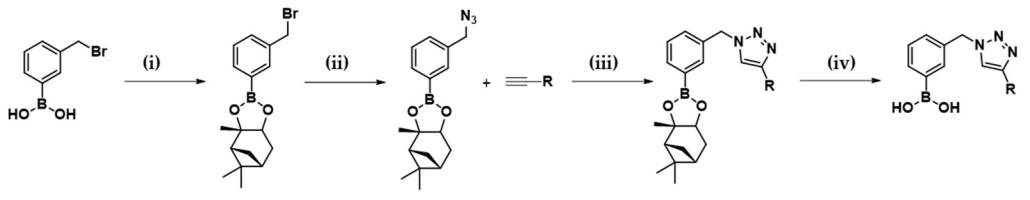

Figure 6. General synthesis for 1,4-derivatives BATSIs. Reagents and conditions: (**i**) *m*-Bromomethylphenyl boronic acid (1.0 eq.), (+)-pinanediol (1.0 eq.), THF, rt, on, quantitative. (**ii**) **15** (1.0 eq.), NaN_3 (10.0 eq.), MeOH, reflux, 5 h, 82%. (**iii**) **16** (1.0 eq.), alkyne (1.0 eq.), $CuSO_4$ (0.05 eq.), Na Ascorbate (0.2 eq.), THPTA (0.05 eq.), *t*-

 doi:10.20944/preprints202503.0489.v1

*Bu*OH:H_2O 1:1, 60 ° C, 1-8 h, 80-99%. (**iv**) Protected triazoles (1.0 eq.), $MeB(OH)_2$ (10.0 eq.), HCl 0.2 M (1.0 eq.), DCM, rt, on, 50-99%.

The ability of the KTGS technique to identify good inhibitors of KPC-2 was evaluated by comparing the K_i values of screened and control compounds against KPC-2. Using a four-step synthesis starting from commercially available *m*-bromomethylphenyl boronic acid, compounds **5-11** were prepared and tested biologically (Figure 7). Compound **7**, selected from the screening with an AC of 5-6, displayed a K_i of 1.7 μM. Compounds **5** and **6**, with ACs of 3-4, exhibited similar inhibitory activity (K_i = 0.73 μM and 0.8 μM, respectively). For both cpds **5** and **6**, a 3-fold improvement compared to the warhead activity (K_i = 2.3 μM) was observed. However, some control compounds, notably compound **11**, showed comparable or superior activity (K_i = 0.46 μM), despite not being identified in the KTGS screening (false negative).

Cpd	Warhead/R group	Product Synthesised	AC	K_i (μM)
3 (Warhead)		-	-	2.3 ± 0.5
5 (Al-32)	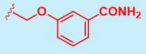	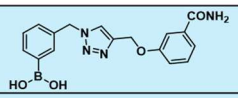	**3-4 (50:50)**	0.73 ± 0.03
6 (Al-39)		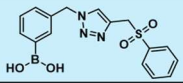	**3-4 (100:0)**	0.8 ± 0.01
7 (Al-57)	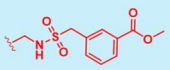	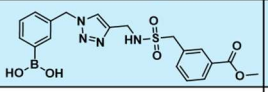	**5-6 (50:50)**	1.7 ± 0.1
8 (Al-2)	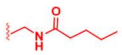	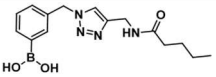	2-3	7.6 ± 0.4
9 (Al-7)		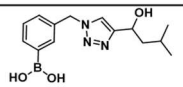	1-2	5.6 ± 0.3
10 (Al-12)		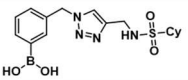	1-2	0.67 ± 0.1
11 (Al-31)		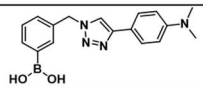	0-1	0.46 ± 0.03

Figure 7. Compounds synthesised and their biological evaluation. AC= Amplification coefficient. In the AC column, between brackets is reported the regioisomeric ratio observed (1,4- vs 1,5-). In light blue are indicate the compounds obtained from the KPC-2 screening. Substrate: Nitrocefin (NCF). K_M (NCF)=16 ± 1.2 μM; [NCF]: 100 μM; [KPC-2]= 67 nM.

2.5. In Situ Click Chemistry with AmpC

The results in Table 1 indicate that warhead **3** completely inhibits AmpC at a concentration of 100 μM, demonstrating a promising target-warhead combination for optimising and enhancing KTGS outcomes. Following the same conditions used for the multicomponent screening with KPC-2, the *in situ* click chemistry experiment was performed using AmpC as template. Similarly, out of 90-potential triazoles, only three products were formed with amplification coefficient >3 (Figure 8). In the first case, cycloaddition of **3** with the alkyne **Al-12** produced regioisomers **10** and **10a** (ratio 21:79) in a ratio between 5 and 6. An acceptable AC was obtained also for **Al-57**, which was transformed into the triazole **7** in 50:50 regioisomeric ratio. Eventually, the 1,5-product of the reaction between the warhead **3** and **Al-88** was also formed with AC 3-4 compared to controls.

 doi:10.20944/preprints202503.0489.v1

Amplification coefficient vs negative controls (No protein and BSA)									
N.F.		0 < AC > 1			1 < AC < 3		AC > 3		
Cluster 1	Cluster 2	Cluster 3	Cluster 4	Cluster 5	Cluster 6	Cluster 7	Cluster 8	Cluster 9	Cluster 10
Al-1	Al-10	Al-19	Al-28	Al-37	Al-46	Al-55	Al-64	Al-73	Al-82
Al-2	Al-11	Al-20	Al-29	Al-38	Al-47	Al-56	Al-65	Al-74	Al-83
Al-3	Al-12	Al-21	Al-30	Al-39	Al-48	Al-57	Al-66	Al-75	Al-84
Al-4	Al-13	Al-22	Al-31	Al-40	Al-49	Al-58	Al-67	Al-76	Al-85
Al-5	Al-14	Al-23	Al-32	Al-41	Al-50	Al-59	Al-68	Al-77	Al-86
Al-6	Al-15	Al-24	Al-33	Al-42	Al-51	Al-60	Al-69	Al-78	Al-87
Al-7	Al-16	Al-25	Al-34	Al-43	Al-52	Al-61	Al-70	Al-79	Al-88
Al-8	Al-17	Al-26	Al-35	Al-44	Al-53	Al-62	Al-71	Al-80	Al-89
Al-9	Al-18	Al-27	Al-36	Al-45	Al-54	Al-63	Al-72	Al-81	Al-90

Figure 8. Cold map for the *in situ* click chemistry screening using AmpC. Each cell corresponds to an alkyne. In dark blue are denoted alkynes that generated triazoles with AC > 3 in presence of the protein template.

Potentially bioactive BATSIs and controls were synthesised following the synthesis reported in Figure 6 (1,4-regioisomers) and Figure 9 (1,5-regioisomers), and characterised. Despite several attempts, the 1,5-product could not be synthesised due to the low catalytic efficiency of the Cp*RuCl(PPh$_3$)$_2$ catalyst used, and only the 1,4-product **12** was successfully obtained.

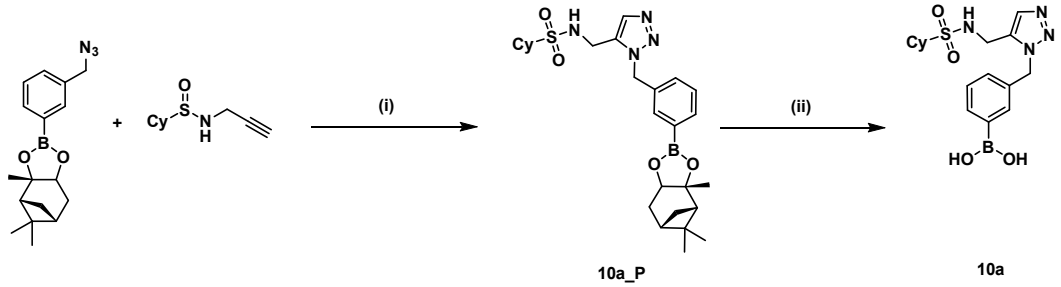

Figure 9. Synthesis for the 1,5-regioisomer **10a**. (i) **16** (1.0 eq.), **Al-12** (1.1 eq.), Cp*RuCl(PPh$_3$)$_2$ (0.025 eq.), THF, 70 ° C, 8 h, 40%. (ii) **10a_P** (1.0 eq.), MeB(OH)$_2$ (10.0 eq.), HCl 0.2 M (1 eq.), DCM, rt, on, 76%.

Microbiological assays with AmpC highlighted the 1,5-regioisomer **10a** (Figure 10, AC 5-6) as the most potent inhibitor, showing a K_i value of 140 nM. The corresponding 1,4-regioisomer **10**, observed at 21% in the screening, displayed nanomolar potency (K_i = 600 nM), yet four-fold weaker with respect to the 1,5-regioisomer. Compounds **7** and **12**, identified with ACs of 4-5 and 3-4 respectively, were also effective inhibitors (K_i = 300 and 400 nM, respectively). Notably, warhead **3** itself exhibited a K_i of 700 nM. Control compounds (cpds **8**, **9**, **11** and **13**) displayed a various range of activity. While controls **8** and **9** exhibited worse inhibitory activity (K_i = 1.5 and 11 μM, respectively) when compared to warhead **3**, cpds **11** and **13** demonstrated similar activity (K_i = 280 and 800 nM, respectively) to the triazoles selected from the AmpC screening.

To assess whether the *in situ* click chemistry takes place within AmpC active site, the following experiment was performed. **SM23**, a known AmpC inhibitor (K_i 1 nM) previously reported by our group,[18,60] was added to the reaction aiming to assess if the catalysis was affected by a BATSI obstructing the target active site (Scheme 2). For this experiment a binary combination between warhead **3** and a model alkyne (**Al-12**) was selected.

In the absence of **SM23**, 20 mol% of AmpC catalyses the formation of both regioisomers **10** and **10a** (Table 2, Entry 3, regioisomeric ratio 21:79) compared to no enzyme (Entry 1) and BSA (Entry 2). As predictable, even 1 mol% of **SM23** in combination of 20 mol% of AmpC affects the ratio of formation of triazoles **10**/**10a**. In this case, AmpC catalyses only the formation of **10a** with AC of 1-2 (Entry 4). An even more dramatic drop in conversion is observed when the amount of **SM23** was equal to the AmpC one, with neither AC>1 nor regioselectivity observed (Entry 5). Therefore, those

 doi:10.20944/preprints202503.0489.v1

findings suggest the *in situ* click chemistry between warhead **3** and alkyne **Al-12** happens within AmpC catalytic site.

Cpd	Warhead/R group	Product Synthesised	AC	K_i (μM)
3 (Warhead)	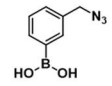	-		0.7 ± 0.03
7 (Al-57)	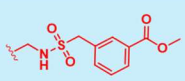	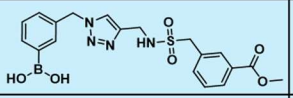	4-5 (50:50)	0.3 ± 0.02
10 (Al-12)		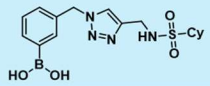	5-6 (21:79)	0.6 ± 0.1
10a (Al-12)		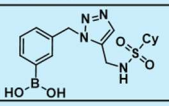	5-6 (21:79)	0.14 ± 0.01
12 (Al-88)	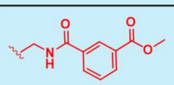	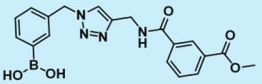	3-4 (0:100)	0.4 ± 0.02
8 (Al-2)	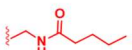	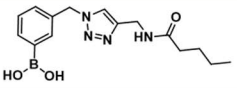	2-3	1.5 ± 0.1
9 (Al-7)		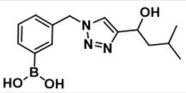	2-3	11 ± 0.2
11 (Al-31)		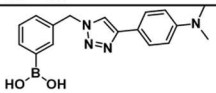	N.F.	0.28 ± 0.05
13 (Al-10)	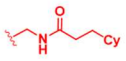	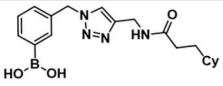	0-1	0.8 ± 0.1

Figure 10. Compounds synthesised and their biological evaluation. AC= Amplification coefficient. In the AC column, between brackets is reported the regioisomeric ratio observed (1,4- vs 1,5-). In light blue are indicate the compounds from the AmpC screening. Substrate: Nitrocefin (NCF). K_M_NCF=118±2 μM; [NCF]: 100 μM; [AmpC]= 36 nM.

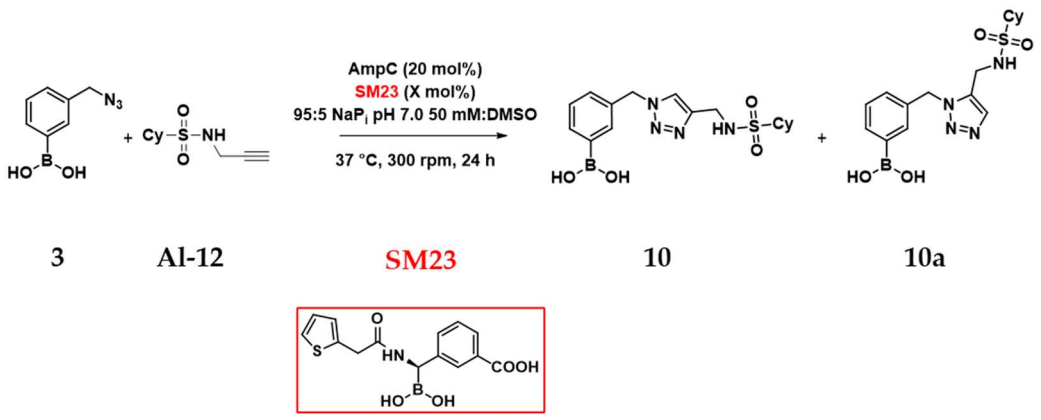

Scheme 2. *In situ* click chemistry between **3** and **Al-12** in presence of AmpC and **SM23** (red box).

Table 2. AmpC catalytic activity in presence of **SM23** inhibitor. AC= Amplification Coefficient.

Entry*	Enzyme	%**SM23**	Regioselectivity (**10**:**10a**)	AC **10/10a**
1	None	-	50:50	-
2	BSA (20 mol%)	-	60:40	-

 doi:10.20944/preprints202503.0489.v1

3	AmpC (20 mol%)	-	21:79	5-6
4	AmpC (20 mol%)	1 mol%	0:100	1-2
5	AmpC (20 mol%)	20 mol%	50:50	0-1

*Reactions were run in 0.2 mL microtubes with a total volume of 100 µL. Conditions: **3** (1 eq.), **Al-12** (5 eq.), 95:5 sodium phosphate 50 mM pH 7.0: DMSO; 300 rpm; 37 °C; 24 h.

Given that boronic acids act as transition-state inhibitors by binding the catalytic serine of β-lactamases through a reversible covalent bond, we aimed to determine whether the *in situ* click chemistry reaction products were quantitatively detected during LC-MS analysis. Although boronic acids are reversible binders, their fast on–slow off behaviour raised concerns that triazole product formation might be underestimated due to covalent adducts forming with the protein target.[61] To investigate this, compound **10a**, warhead **3**, and compounds **8** and **9** were incubated with AmpC (1:1 or 1:5 protein:compound ratio), and their detection was monitored over 24 hours. The selection of these compounds was designed to assess whether potent inhibitors (e.g., compound **10a**, K_i = 140 nM) had a different impact compared to less effective scaffolds (e.g., compound **9**, K_i = 11 µM). The percentage of boronic acids detected was estimated using peak area measurements in LC-MS targeted SIM mode, with quantification performed using calibration curves. The experiments were conducted at 37 °C in a 95:5 sodium phosphate 50 mM pH 7.0:DMSO mixture.

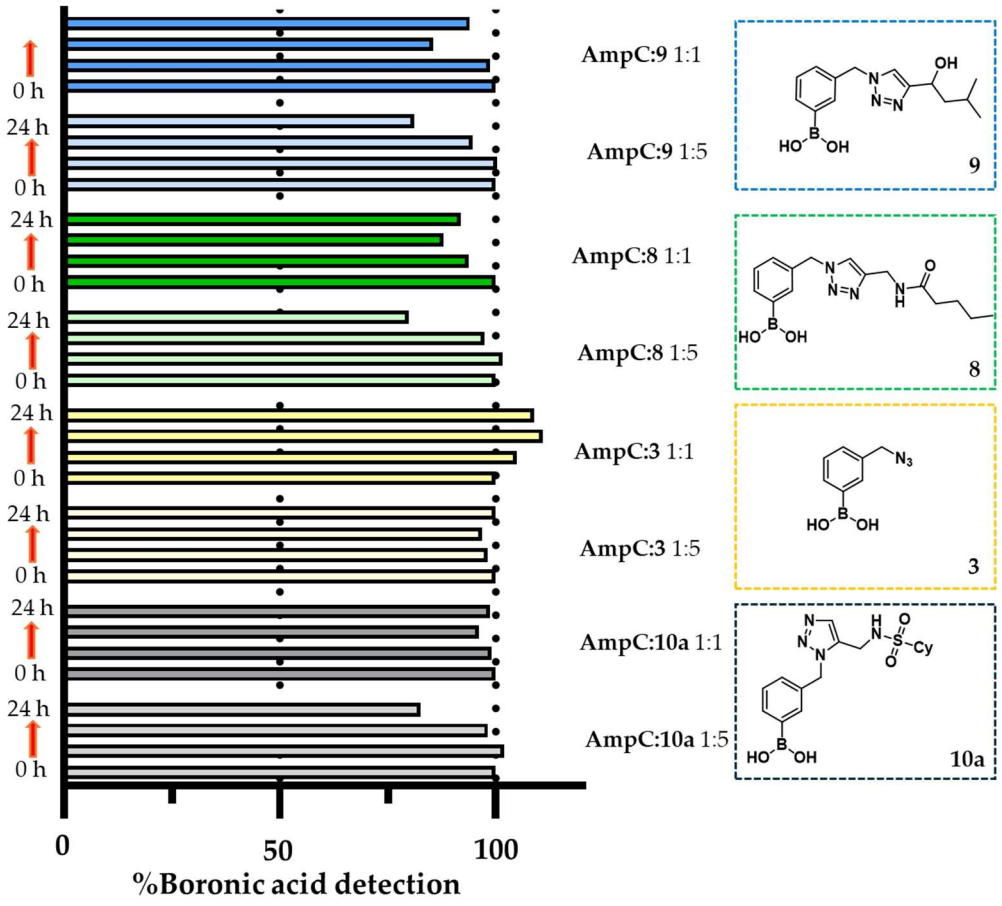

Figure 7. % of detection of **10a** (grey box), **3** (yellow box), **8** (green box) and **9** (blue box) over the course of the 24 h using t-SIM method. Each cpd was tested in presence of 20% mol of AmpC or stoichiometric amount of AmpC. Each box includes 4 columns corresponding to % boronic acid detected at a certain time point (0, 8, 16 and 24 h).

For compound **10a**, the most potent AmpC inhibitor reported in this study, a slight decrease in detection was observed over 24 hours, with 83% of **10a** remaining in the presence of 20 mol% of the

 doi:10.20944/preprints202503.0489.v1

target protein. However, when **10a** and AmpC were incubated at a stoichiometric ratio, **10a** levels remained stable throughout the experiment. A similar trend was observed for compounds **8** and **9**, indicating that the inhibitors affinity for the protein target did not influence its detection in the LC-MS analysis. Additionally, no differences were observed when warhead **3** was incubated with either a limiting or stoichiometric amount of AmpC. These findings suggest that the covalent nature of the warhead and the *in situ* click chemistry products did not interfere with the KTGS experiments or their outcomes.

3. Discussion

In this work, we investigated whether in *situ* click chemistry can be readily employed as a platform to discover boronic acid-based β-lactamase inhibitors. Previously, triazole-containing boronic compounds were discovered following standard procedures (CuAAC) on mgs scale leading to the discovery of potent β-lactamase inhibitors.[17] In contrast, the synthesis of inhibitors within the catalytic site of an enzyme using a multicomponent assay offers different advantages. Firstly, this approach is timesaving, since 90 reactions can potentially be conducted simultaneously, allowing a rapid identification of inhibitors. A second advantage is operability, as the boronic group contained in the warhead does not require tedious protection and deprotection steps, which are often required when a click reaction is conducted under conditions of chemical catalysis with Cu(I). Eventually, small-scale reactions represent an economically viable solution for avoiding an excessive consumption of reagents. In this study, two enzymes belonging to separate classes of β-lactamases were used as template, the class A carbapenemase KPC-2 and the class C cephalosporinase AmpC. Despite sharing the same mechanism of action, those enzymes possess different specificity towards β-lactam antibiotics, reflecting the diversity of their catalytic sites. Analysis on KPC-2 and AmpC active sites with Dog Site Scorer, an automated tool able to predict and evaluate binding pockets for druggability assessment, reveals significant differences on the physicochemical properties of the two target pockets chemistry (see SI Table S4 and figures S11-S14).[52] While KPC-2 possess a narrow and enclosed active site, suggesting a lower pre-disposition to accommodate KTGS building blocks, AmpC, display larger volume, broader surface, and favourable physicochemical parameters.

Microbiological screening of the azidomethylphenyl boronic warheads designed revealed boronic warhead 3, bearing the substituent in the *meta* position, as the most active towards both KPC-2 and Amp-C. When the *in situ* click chemistry experiment was conducted in presence of those enzymes, few alkynes were selected for the formation of the triazoles, indicating that both β-lactamases can catalyse the azido-alkyne cycloaddition reaction. Catalysis in the presence of KPC-2 reveals the formation of three out of 90 potential triazoles with an amplification coefficient > 3 relative to controls. When *in situ* click chemistry is repeated with AmpC, whose catalytic site exhibit more favourable druggability parameters than KPC-2, results are comparable in both amplification coefficient and number of hits. Interestingly, in some cases AmpC dictates a specific preference for the formation of 1,5-regioisomer triazoles (*i.e.* with Al-12 and Al-88).

These results further demonstrate that overcoming the energy barrier typical of the cycloaddition reaction is possible only with appropriate spatial orientation in the catalytic site of both azide and alkyne. To prove that click chemistry takes place within the catalytic site, a binary experiment was attempted with warhead 3 and alkyne Al-12 in the presence of SM23, a potent AmpC inhibitor (K_i = 1 nM). At a concentration of 1 mol% inhibitor, the AC drops from a value of 5-6 without inhibitor, to a value of 1-2. With an equimolar concentration of SM23 and enzyme (20%), a negligible triazole peak is visible, suggesting the high affinity of the inhibitor for the catalytic site prevents the appropriate spatial arrangement of azidoboronate and alkyne for cycloaddition. These combinations of results prove the role of β-lactamases in promoting cycloaddition reaction within their active site. Further control experiments confirmed that both the warhead and reaction products were efficiently detected during LC-MS analysis when incubated with AmpC. This suggests that the reversible covalent bond between the boronic acid and the β-lactamase catalytic serine does not interfere with the quantification of the *in situ* click chemistry products. For both KPC-2 and AmpC, the synthesised

 doi:10.20944/preprints202503.0489.v1

triazoles prove to be better inhibitors than warhead 3 (K_i vs KPC-2 = 2.3 μM; K_i vs AmpC = 700 nM), reaching values of K_i = 730 nM for compound 5, the best KPC-2 inhibitor, and K_i = 140 nM for 10a the best AmpC inhibitor.

Triazole-based BATSIs derived from the reaction of other alkynes that were not selected *in situ*, were also synthesised and tested. Some of them proved to be comparable inhibitors as the hit compounds against both enzymes, suggesting how this technique can un-detect potential inhibitors. This problem of "false negative", however, is inherent in the technique itself.[49-51,62] Furthermore, structural rigidity and steric constraints of the boronic acid scaffold likely restricted the conformational freedom required for effective alignment of reactants. While the reversible covalent interaction between the catalytic serine and the electrophilic boron anchors the warhead within the active site, it also limits the spatial and conformational flexibility needed for alkyne fragments. These limitations emphasise the necessity of designing more flexible and adaptable warheads, such as warhead 1, that might balance inherent activity with catalytic efficiency for inhibitors formation through KTGS applications.

4. Materials and Methods

4.1. Chemistry

Methods. All reactions dealing with[49–51,62 air- and moisture-sensitive compounds were carried out in dry reaction vessels under a nitrogen atmosphere. Flash column chromatography (CC) was performed using silica gels (particle size 35-70 μm). Solvents used in CC were commercially available and distilled before use. Thin layer chromatography was used for product detection using silica gel-coated plates, with visualization effected via exposure to UV Light at 254 nm or staining and heating with potassium permanganate ($KMnO_4$) or Pancaldi solution (phosphomolybdic acid and Ce(IV)sulphate in 4% sulphuric acid).

Instrumentation. ^{1}H NMR, ^{13}C NMR and ^{11}B NMR spectra were obtained on a Bruker Ascend 400 at 400 MHz (^{1}H NMR at 400 MHz, ^{13}C NMR at 101 MHz, ^{11}B NMR at 128 MHz) and Bruker Ascend 600 at 600 MHz (^{1}H NMR at 600 MHz, ^{13}C NMR at 151 MHz, ^{11}B NMR at 193 MHz) at ambient temperature with $CDCl_3$, CD_3OD, D_2O or d_6-DMSO as deuterated solvent. All chemical shifts δ are reported in parts per million (ppm), and the residual solvent peak was used as an internal reference: proton ($CDCl_3$ δ 7.26, MeOD δ 3.31, D_2O δ 4.79, DMSO δ 2.50), carbon ($CDCl_3$ δ 77.0, MeOD δ 49.0, DMSO δ 39.5), or tetramethylsilane (TMS δ 0.00) were used as a reference. Coupling constants (J) were reported in Hertz (Hz) and referred to apparent peak multiplets. Data for ^{1}H NMR spectra were reported as follows: chemical shift (ppm), multiplicity (given as s(singlet), d (doublet), t (triplet), q (quartet), m (multiplet), br (broad) or a combination of them), coupling constants (Hz) and integration. ^{13}C NMR and ^{11}B NMR were only reported as chemical shifts. High-resolution mass spectra (HRMS) were recorded on a Ultimate 3000 UHPLC coupled to a Q-Exactive hybrid quadrupole-Orbitrap mass spectrometer via a heated electrospray ionization source HESI-II (Thermo Fisher Scientific).

Materials. All reagents and solvents were of commercial quality from freshly opened containers. All substances that are not described in the following synthetic procedures were obtained from commercial suppliers (BLD pharm, Merck, Fisher scientific, Santacruz biotechnology and Enamine). Anhydrous 1,4-dioxane, toluene, and other solvents were purchased and used under N_2 atmosphere.

Synthesis and characterisation data. Detailed synthetic procedures, compounds characterisation and spectral data are available in the supplementary materials.

4.2. In Situ Click Chemistry

Materials. Reactions were incubated in a TS-100C (Biosan) thermo-shaker equipped with an interchangeable heating block for microtubes and PCR plates.

Cluster of alkynes preparation. Mixtures of alkynes (cluster 1 to 10, see Figure 4) were prepared from a dimethylsulfoxide (DMSO) 50 mM stock solution of each alkyne: mixtures X (10 clusters of 9

 doi:10.20944/preprints202503.0489.v1

alkynes): mixing 10 µL of DMSO to 10 µL of stock solutions of 9 alkynes to reach 5 mM final concentration of each alkyne.

Azide preparation. Warhead 3 was dissolved in DMSO at 50 mM final concentration. For reactions, warhead 3 was diluted to 1 mM in DMSO.

Binary and multicomponent KTGS. In a 0.2 mL microtube were mixed 2.5 µL of azide 3 (stock concentration of 1 mM in DMSO), 2.5 µL of an alkyne mixture (stock 5 mM in DMSO), 6.9 µL of AmpC (stock 72 µM in NaP_i pH 7.0) and 88.1 µL of 50 mM sodium phosphate buffer pH 7.0 to reach a final volume of 100 µL. Final concentrations are the following: azide 25 µM (1 eq.), alkyne cluster 125 µM (5 eq.x9), AmpC 5 µM (20 mol% or 0.02 eq.), DMSO 5%. For experiments in presence of KPC-2, 3.27 µL of KPC-2 (stock 153 µM in NaP_i pH 7.0) were used to afford a final concentration of 5 µM (20 mol% or 0.02 eq.). The microtube was shaken at 300 rpm at 37°C for 24 h. Reactions were transferred into a LC-MS vial and directly injected (10 µL) for liquid chromatography–mass spectrometry (LC–MS). Reactions were analysed with an Ultimate 3000 UHPLC coupled to a Q-Exactive hybrid quadrupole-Orbitrap mass spectrometer via a heated electrospray ionization source HESI-II. The chromatographic separation was performed injecting a 10 µL sample volume on a Hypersil Gold C18 100 x 2.1 mm, 1.9 µm column (Thermo Fisher Scientific) kept at 30 °C eluting with 0.3 mL/min flow of ultrapure water (A) and methanol (B) both with 0.1% formic acid as mobile phase. A linear gradient profile was applied from 2% to 98% B over 10 min followed by a reconditioning step pending successive sample injection. A data-dependent mass spectrometric data acquisition strategy was used for (Full MS/DD-MS2). Full MS experiments were acquired alternating positive and negative ionization mode at 35000 FWHM (at 200 m/z) resolving power with a 250<m/z<1000 scan range and AGC target and maximum injection time set at $3e^6$ and 243 ms respectively. Top 2 mono-charged ions were selected for MS2 acquisition at 17500 FWHM using a 4.3 m/z (1.0 offset) wide isolation window, with AGC at $2e^5$ and 100 ms maximum injection time. An inclusion list was eventually used to target MS2 spectra acquisition of preferred ion species. Detection was based on calculated $[M+H]^+$ and $[M-H]^-$ molecular ions with a 5 ppm accuracy tolerance for their respective ion chromatogram extraction. Peak retention time and area of detected target compounds was used for their detection and semi-quantitative evaluation in between reaction batches.

For controls (buffer and BSA), AmpC/KPC-2 is replaced with no enzyme (buffer volume 95 µL) and BSA (stock 100 µM, final concentration 5 µM, buffer volume 90 µL). Hits were identified in each cluster by mass and retention time and compared to both controls (buffer and BSA) and synthetically prepared triazoles obtained in mixtures. Peak area of each triazole obtained in presence of the proteins (AmpC and KPC-2) was compared to the peaks observed with controls to calculate the amplification coefficient (AC, $PA_{KPC\text{-}2/AmpC}$/ $PA_{No\ protein/BSA}$).

CuAAC positive controls. In a 0.2 mL microtube were mixed 2.5 µL of azide 3 (stock concentration of 1 mM in DMSO), 2.5 µL of an alkyne mixture (stock 5 mM in DMSO), 2.5 µL of $CuSO_4$ (stock 1 mM in water), 2.5 µL of sodium ascorbate (stock 5 mM in water) 2.5 µL of THPTA (stock 2 mM in water), 40 µL of water and 47.5 µL of *t-Bu*OH to reach a final volume of 100 µL. Final concentrations are the following: azide 25 µM (1 eq.), alkyne cluster 125 µM (5 eq.x9), $CuSO_4$ 25 µM (1 eq.), sodium ascorbate 125 µM (5 eq.), THPTA 50 µM (2 eq.), DMSO 5%, *t-Bu*OH 47.5 %, water 47.5%. The microtube was shaken at 300 rpm at 37°C for 24 h. Reactions were transferred into a LC-MS vial and analysed in the same way described in the Binary and multicomponent KTGS section above.

Thermal reactions. In a 0.2 mL microtube were mixed 2.5 µL of azide 3 (stock concentration of 1 mM in DMSO), 2.5 µL of an alkyne mixture (stock 5.1 mM in DMSO), and 95 µL of 50 mM sodium phosphate buffer pH 7.0 to reach a final volume of 100 µL. Final concentrations are the following: azide 25 µM (1 eq.), alkyne cluster 125 µM (5 eq.x9). The microtube was shaken at 300 rpm at 80°C for 24 h. Reactions were transferred into a LC-MS vial and analysed in the same way described in the Binary and multicomponent KTGS section above.

 doi:10.20944/preprints202503.0489.v1

4.3. Microbiology and Determination of K_i

B-lactamases used in the present study were from a Clinical Biochemistry Laboratory collection (Department of Biotechnological and Applied Clinical Sciences, University of L'Aquila, L'Aquila, Italy). All enzymes show a purity degree higher than 95%. Concentration of each enzyme was determined by Bradford assay. The K_M values of each β-lactamase for nitrocefin were determined following the hydrolysis of substrate under the initial rate and by linearization of Michaelis-Menten equation using Hanes-Woolf method.[63]

Competitive inhibition assays were monitored directly using, as reporter substrate, 100 μM nitrocefin. K_i values were calculated using the following equation:

$$v_0/v_i=1+ (K_M \times I)/(K_M +S) \times K_i,$$

where v_i and v_0 are the initial rates of hydrolysis of nitrocefin with or without inhibitor, respectively; I is the concentration of inhibitor, K_i is the inhibition constant, K_M is the Michaelis-Menten constant, and S is the concentration of reporter substrate. The plot v_0/v_i versus [I] yielded a straight line of slope $K_M/(K_M+S) \times K_i$.[64]

The IC_{50} value for each compound was graphically calculated plotting residual activity (%) versus [I].

For the β-lactamases test at a fixed concentration reported in Table 1 the following conditions were applied:

β-lactamase	Buffer	Substrate	$K_{M\ substrate}$	[Substrate]	[β-lactamase]
KPC-2	NaPi[1]	NCF[3]	10 ± 1 μM	50 μM	1 nM
CTX-M-15	NaPi	NCF	35 ± 1 μM	25 μM	2.5 nM
KPC-53	NaPi	NCF	106 ± 2 μM	100 μM	30 nM
SHV-12	NaPi	NCF	50 ± 3 μM	25 μM	7 nM
NDM-1	HEPES[2]	MPM[4]	80 ± 1 μM	100 μM	4.5 nM
VIM-1	HEPES	MPM	130 ± 4 μM	150 μM	22 nM
IMP-1	HEPES	MPM	30 ± 1 μM	80 μM	13 nM
AmpC	NaPi	NCF	118 ± 2 μM	142 μM	14 nM
ADC-25	NaPi	NCF	120 ± 3 μM	24 μM	3 nM
CMY-2	NaPi	NCF	8 ± 1 μM	24 μM	2.5 nM
OXA-24	NaPi	NCF	29 ± 1 μM	142 μM	4 nM
OXA-48	NaPi	IMI[5]	13 ± 1 μM	50 μM	75 nM

[1] NaPi 50 mM pH 7.0; [2] HEPES 20 mM pH 7.0+ 20 μM Zn. [3] NCF = Nitrocefin; [4] MPM = Meropenem; [5] IMI = Imipenem.

Supplementary Materials: The following supporting information can be downloaded at: Preprints.org.

Author Contributions: Conceptualization, N.S., E.C. and F.P; methodology, N.S, A.P., M.P. and E.C.; validation, N.S, A.P., M.P. and E.C.; formal analysis, N.S, A.P., M.P. and E.C.; investigation, N.S, A.P. and M.P.; resources, N.S., A.P., M.P., R.B., F.F., E.C. and F.P.; data curation, N.S, A.P. and M.P.; writing—original draft preparation, N.S., E.C. and F.P; writing—review and editing, , N.S., A.P., M.P., R.B., F.F., E.C. and F.P.; visualization, N.S.; supervision, N.S., E.C. and F.P.; funding acquisition, N.S., M.P., R.B., E.C. and F.P.. All authors have read and agreed to the published version of the manuscript.

Funding: Funded by the European Union. Views and opinions expressed are however those of the author(s) only and do not necessarily reflect those of the European Union or other granting authority. Neither the European Union nor the granting authority can be held responsible for them. This project has received funding from the European Union's Horizon Europe research and innovation programme under the Marie Sklodowska-Curie grant agreement no. 101068156. Further information can be found on the website: https://www.bliss.unimore.it/. This study was also partially supported by funds provided by the Ministry of University and Research of Italy (MIUR)- PRIN-2022, Project Number: 2022WBPFSC. This research was also supported by the National Institute of Allergy and Infectious Diseases of the National Institutes of Health (NIH) under award number R01AI072219 (to RAB, FP, and EC), and in part by funds and/or facilities provided by the Cleveland Department of Veterans Affairs, Award Number I01BX001974 to RAB from the Biomedical Laboratory Research & Development Service of the VA Office of Research and Development. The content is

 doi:10.20944/preprints202503.0489.v1

solely the responsibility of the authors and does not necessarily represent the official views of the NIH or the Department of Veterans Affairs.

Data Availability Statement: The original contributions presented in this study are included in the article/supplementary material. Further inquiries can be directed to the corresponding author.

Acknowledgments: We would like to extend our gratitude to Prof Alejandro J. Vila for the precious support and suggestions. His expertise has greatly benefited the study. We would like to extend our gratitude to Dr Diego Pinetti and all the Centro Interdipartimentale Grandi Strumenti (CIGS, UNIMORE) for the great support throughout all the experiment performed.

Conflicts of Interest: The authors declare no conflicts of interest. The funders had no role in the design of the study; in the collection, analyses, or interpretation of data; in the writing of the manuscript; or in the decision to publish the results.

References

1. Tang, S.S.; Apisarnthanarak, A.; Hsu, L.Y. Mechanisms of β-lactam antimicrobial resistance and epidemiology of major community- and healthcare-associated multidrug-resistant bacteria. *Advanced Drug Delivery Reviews* **2014**, *78*, 3-13, doi:https://doi.org/10.1016/j.addr.2014.08.003.
2. Lima, L.M.; Silva, B.N.M.d.; Barbosa, G.; Barreiro, E.J. β-lactam antibiotics: An overview from a medicinal chemistry perspective. *European Journal of Medicinal Chemistry* **2020**, *208*, 112829, doi:https://doi.org/10.1016/j.ejmech.2020.112829.
3. Docquier, J.-D.; Mangani, S. An update on β-lactamase inhibitor discovery and development. *Drug Resistance Updates* **2018**, *36*, 13-29, doi:https://doi.org/10.1016/j.drup.2017.11.002.
4. Zhang, S.; Liao, X.; Ding, T.; Ahn, J. Role of β-Lactamase Inhibitors as Potentiators in Antimicrobial Chemotherapy Targeting Gram-Negative Bacteria. *Antibiotics* **2024**, *13*, doi:10.3390/antibiotics13030260.
5. Munita Jose, M.; Arias Cesar, A. Mechanisms of Antibiotic Resistance. *Microbiology Spectrum* **2016**, *4*, 10.1128/microbiolspec.vmbf-0016-2015, doi:10.1128/microbiolspec.vmbf-0016-2015.
6. Darby, E.M.; Trampari, E.; Siasat, P.; Gaya, M.S.; Alav, I.; Webber, M.A.; Blair, J.M.A. Molecular mechanisms of antibiotic resistance revisited. *Nature Reviews Microbiology* **2023**, *21*, 280-295, doi:10.1038/s41579-022-00820-y.
7. Hall, B.G.; Barlow, M. Revised Ambler classification of β-lactamases. *Journal of Antimicrobial Chemotherapy* **2005**, *55*, 1050-1051, doi:10.1093/jac/dki130.
8. Tooke, C.L.; Hinchliffe, P.; Bragginton, E.C.; Colenso, C.K.; Hirvonen, V.H.A.; Takebayashi, Y.; Spencer, J. β-Lactamases and β-Lactamase Inhibitors in the 21st Century. *Journal of Molecular Biology* **2019**, *431*, 3472-3500, doi:https://doi.org/10.1016/j.jmb.2019.04.002.
9. Bush, K.; Jacoby George, A. Updated Functional Classification of β-Lactamases. *Antimicrobial Agents and Chemotherapy* **2010**, *54*, 969-976, doi:10.1128/AAC.01009-09.
10. Hall, B.G.; Barlow, M. Evolution of the serine β-lactamases: past, present and future. *Drug Resistance Updates* **2004**, *7*, 111-123, doi:https://doi.org/10.1016/j.drup.2004.02.003.
11. Bradford Patricia, A. Extended-Spectrum β-Lactamases in the 21st Century: Characterization, Epidemiology, and Detection of This Important Resistance Threat. *Clinical Microbiology Reviews* **2001**, *14*, 933-951, doi:10.1128/CMR.14.4.933-951.2001.
12. Castanheira, M.; Simner, P.J.; Bradford, P.A. Extended-spectrum β-lactamases: an update on their characteristics, epidemiology and detection. *JAC-Antimicrobial Resistance* **2021**, *3*, dlab092, doi:10.1093/jacamr/dlab092.
13. Hammoudi Halat, D.; Ayoub Moubareck, C. The Current Burden of Carbapenemases: Review of Significant Properties and Dissemination among Gram-Negative Bacteria. *Antibiotics* **2020**, *9*, doi:10.3390/antibiotics9040186.
14. Bedenic, B.; Plecko, V.; Sardelic, S.; Uzunovic, S.; Torkar, K.G. Carbapenemases in Gram-Negative Bacteria: Laboratory Detection and Clinical Significance. *BioMed Research International* **2014**, *2014*, doi:https://doi.org/10.1155/2014/841951.
15. Codjoe, F.S.; Donkor, E.S. Carbapenem Resistance: A Review. *Medical Sciences* **2018**, *6*, doi:10.3390/medsci6010001.

16. Bush, K.; Bradford, P.A. Interplay between β-lactamases and new β-lactamase inhibitors. *Nature Reviews Microbiology* **2019**, *17*, 295-306, doi:10.1038/s41579-019-0159-8.
17. Caselli, E.; Romagnoli, C.; Vahabi, R.; Taracila, M.A.; Bonomo, R.A.; Prati, F. Click Chemistry in Lead Optimization of Boronic Acids as β-Lactamase Inhibitors. *Journal of Medicinal Chemistry* **2015**, *58*, 5445-5458, doi:10.1021/acs.jmedchem.5b00341.
18. Caselli, E.; Romagnoli, C.; Powers, R.A.; Taracila, M.A.; Bouza, A.A.; Swanson, H.C.; Smolen, K.A.; Fini, F.; Wallar, B.J.; Bonomo, R.A.; et al. Inhibition of Acinetobacter-Derived Cephalosporinase: Exploring the Carboxylate Recognition Site Using Novel β-Lactamase Inhibitors. *ACS Infectious Diseases* **2018**, *4*, 337-348, doi:10.1021/acsinfecdis.7b00153.
19. Ishikawa, T.; Furukawa, N.; Caselli, E.; Prati, F.; Taracila, M.A.; Bethel, C.R.; Ishii, Y.; Shimizu-Ibuka, A.; Bonomo, R.A. Insights Into the Inhibition of MOX-1 β-Lactamase by S02030, a Boronic Acid Transition State Inhibitor. *Frontiers in Microbiology* **2021**, *12*, doi:10.3389/fmicb.2021.720036.
20. Rojas, L.J.; Taracila, M.A.; Papp-Wallace, K.M.; Bethel, C.R.; Caselli, E.; Romagnoli, C.; Winkler, M.L.; Spellberg, B.; Prati, F.; Bonomo, R.A. Boronic Acid Transition State Inhibitors Active against KPC and Other Class A β-Lactamases: Structure-Activity Relationships as a Guide to Inhibitor Design. *Antimicrobial Agents and Chemotherapy 60*, 1751-1759, doi:10.1128/AAC.02641-15.
21. Winkler, M.L.; Rodkey, E.A.; Taracila, M.A.; Drawz, S.M.; Bethel, C.R.; Papp-Wallace, K.M.; Smith, K.M.; Xu, Y.; Dwulit-Smith, J.R.; Romagnoli, C.; et al. Design and Exploration of Novel Boronic Acid Inhibitors Reveals Important Interactions with a Clavulanic Acid-Resistant Sulfhydryl-Variable (SHV) β-Lactamase. *Journal of Medicinal Chemistry* **2013**, *56*, 1084-1097, doi:10.1021/jm301490d.
22. Hamrick Jodie, C.; Docquier, J.-D.; Uehara, T.; Myers Cullen, L.; Six David, A.; Chatwin Cassandra, L.; John Kaitlyn, J.; Vernacchio Salvador, F.; Cusick Susan, M.; Trout Robert, E.L.; et al. VNRX-5133 (Taniborbactam), a Broad-Spectrum Inhibitor of Serine- and Metallo-β-Lactamases, Restores Activity of Cefepime in Enterobacterales and Pseudomonas aeruginosa. *Antimicrobial Agents and Chemotherapy* **2020**, *64*, 10.1128/aac.01963-01919, doi:10.1128/aac.01963-19.
23. Krajnc, A.; Brem, J.; Hinchliffe, P.; Calvopiña, K.; Panduwawala, T.D.; Lang, P.A.; Kamps, J.J.A.G.; Tyrrell, J.M.; Widlake, E.; Saward, B.G.; et al. Bicyclic Boronate VNRX-5133 Inhibits Metallo- and Serine-β-Lactamases. *Journal of Medicinal Chemistry* **2019**, *62*, 8544-8556, doi:10.1021/acs.jmedchem.9b00911.
24. Liu, B.; Trout, R.E.L.; Chu, G.-H.; McGarry, D.; Jackson, R.W.; Hamrick, J.C.; Daigle, D.M.; Cusick, S.M.; Pozzi, C.; De Luca, F.; et al. Discovery of Taniborbactam (VNRX-5133): A Broad-Spectrum Serine- and Metallo-β-lactamase Inhibitor for Carbapenem-Resistant Bacterial Infections. *Journal of Medicinal Chemistry* **2020**, *63*, 2789-2801, doi:10.1021/acs.jmedchem.9b01518.
25. Wagenlehner Florian, M.; Gasink Leanne, B.; McGovern Paul, C.; Moeck, G.; McLeroth, P.; Dorr, M.; Dane, A.; Henkel, T. Cefepime–Taniborbactam in Complicated Urinary Tract Infection. *New England Journal of Medicine* **2024**, *390*, 611-622, doi:10.1056/NEJMoa2304748.
26. Hecker, S.J.; Reddy, K.R.; Lomovskaya, O.; Griffith, D.C.; Rubio-Aparicio, D.; Nelson, K.; Tsivkovski, R.; Sun, D.; Sabet, M.; Tarazi, Z.; et al. Discovery of Cyclic Boronic Acid QPX7728, an Ultrabroad-Spectrum Inhibitor of Serine and Metallo-β-lactamases. *Journal of Medicinal Chemistry* **2020**, *63*, 7491-7507, doi:10.1021/acs.jmedchem.9b01976.
27. Tsivkovski, R.; Totrov, M.; Lomovskaya, O. Biochemical Characterization of QPX7728, a New Ultrabroad-Spectrum Beta-Lactamase Inhibitor of Serine and Metallo-Beta-Lactamases. *Antimicrobial Agents and Chemotherapy 64*, e00130-00120, doi:10.1128/AAC.00130-20.
28. Jacobs, L.M.C.; Consol, P.; Chen, Y. Drug Discovery in the Field of β-Lactams: An Academic Perspective. *Antibiotics* **2024**, *13*, doi:10.3390/antibiotics13010059.
29. Powers, R.A.; Caselli, E.; Focia, P.J.; Prati, F.; Shoichet, B.K. Structures of Ceftazidime and Its Transition-State Analogue in Complex with AmpC β-Lactamase: Implications for Resistance Mutations and Inhibitor Design. *Biochemistry* **2001**, *40*, 9207-9214, doi:10.1021/bi0109358.
30. Drawz, S.M.; Babic, M.; Bethel, C.R.; Taracila, M.; Distler, A.M.; Ori, C.; Caselli, E.; Prati, F.; Bonomo, R.A. Inhibition of the Class C β-Lactamase from Acinetobacter spp.: Insights into Effective Inhibitor Design. *Biochemistry* **2010**, *49*, 329-340, doi:10.1021/bi9015988.

 doi:10.20944/preprints202503.0489.v1

31. Ke, W.; Sampson Jared, M.; Ori, C.; Prati, F.; Drawz Sarah, M.; Bethel Christopher, R.; Bonomo Robert, A.; van den Akker, F. Novel Insights into the Mode of Inhibition of Class A SHV-1 β-Lactamases Revealed by Boronic Acid Transition State Inhibitors. *Antimicrobial Agents and Chemotherapy* **2011**, *55*, 174-183, doi:10.1128/AAC.00930-10.
32. Eidam, O.; Romagnoli, C.; Caselli, E.; Babaoglu, K.; Pohlhaus, D.T.; Karpiak, J.; Bonnet, R.; Shoichet, B.K.; Prati, F. Design, Synthesis, Crystal Structures, and Antimicrobial Activity of Sulfonamide Boronic Acids as β-Lactamase Inhibitors. *Journal of Medicinal Chemistry* **2010**, *53*, 7852-7863, doi:10.1021/jm101015z.
33. Caselli, E.; Fini, F.; Introvigne, M.L.; Stucchi, M.; Taracila, M.A.; Fish, E.R.; Smolen, K.A.; Rather, P.N.; Powers, R.A.; Wallar, B.J.; et al. 1,2,3-Triazolylmethaneboronate: A Structure Activity Relationship Study of a Class of β-Lactamase Inhibitors against Acinetobacter baumannii Cephalosporinase. *ACS Infectious Diseases* **2020**, *6*, 1965-1975, doi:10.1021/acsinfecdis.0c00254.
34. Introvigne, M.L.; Taracila, M.A.; Prati, F.; Caselli, E.; Bonomo, R.A. α-Triazolylboronic Acids: A Promising Scaffold for Effective Inhibitors of KPCs. *ChemMedChem* **2020**, *15*, 1283-1288, doi:https://doi.org/10.1002/cmdc.202000126.
35. Powers, R.A.; June, C.M.; Fernando, M.C.; Fish, E.R.; Maurer, O.L.; Baumann, R.M.; Beardsley, T.J.; Taracila, M.A.; Rudin, S.D.; Hujer, K.M.; et al. Synthesis of a Novel Boronic Acid Transition State Inhibitor, MB076: A Heterocyclic Triazole Effectively Inhibits Acinetobacter-Derived Cephalosporinase Variants with an Expanded-Substrate Spectrum. *Journal of Medicinal Chemistry* **2023**, *66*, 8510-8525, doi:10.1021/acs.jmedchem.3c00144.
36. Nguyen, N.Q.; Krishnan, N.P.; Rojas, L.J.; Prati, F.; Caselli, E.; Romagnoli, C.; Bonomo, R.A.; van den Akker, F. Crystal Structures of KPC-2 and SHV-1 β-Lactamases in Complex with the Boronic Acid Transition State Analog S02030. *Antimicrobial Agents and Chemotherapy 60*, 1760-1766, doi:10.1128/AAC.02643-15.
37. Neumann, S.; Biewend, M.; Rana, S.; Binder, W.H. The CuAAC: Principles, Homogeneous and Heterogeneous Catalysts, and Novel Developments and Applications. *Macromolecular Rapid Communications* **2020**, *41*, 1900359, doi:https://doi.org/10.1002/marc.201900359.
38. Zhao, R.; Zhu, J.; Jiang, X.; Bai, R. Click chemistry-aided drug discovery: A retrospective and prospective outlook. *European Journal of Medicinal Chemistry* **2024**, *264*, 116037, doi:https://doi.org/10.1016/j.ejmech.2023.116037.
39. Bosc, D.; Camberlein, V.; Gealageas, R.; Castillo-Aguilera, O.; Deprez, B.; Deprez-Poulain, R. Kinetic Target-Guided Synthesis: Reaching the Age of Maturity. *Journal of Medicinal Chemistry* **2020**, *63*, 3817-3833, doi:10.1021/acs.jmedchem.9b01183.
40. Bhardwaj, A.; Kaur, J.; Wuest, M.; Wuest, F. In situ click chemistry generation of cyclooxygenase-2 inhibitors. *Nature Communications* **2017**, *8*, 1, doi:10.1038/s41467-016-0009-6.
41. Whiting, M.; Muldoon, J.; Lin, Y.-C.; Silverman, S.M.; Lindstrom, W.; Olson, A.J.; Kolb, H.C.; Finn, M.G.; Sharpless, K.B.; Elder, J.H.; et al. Inhibitors of HIV-1 Protease by Using In Situ Click Chemistry. *Angewandte Chemie International Edition* **2006**, *45*, 1435-1439, doi:https://doi.org/10.1002/anie.200502161.
42. Hirose, T.; Sunazuka, T.; Sugawara, A.; Endo, A.; Iguchi, K.; Yamamoto, T.; Ui, H.; Shiomi, K.; Watanabe, T.; Sharpless, K.B.; et al. Chitinase inhibitors: extraction of the active framework from natural argifin and use of in situ click chemistry. *The Journal of Antibiotics* **2009**, *62*, 277-282, doi:10.1038/ja.2009.28.
43. Grimster, N.P.; Stump, B.; Fotsing, J.R.; Weide, T.; Talley, T.T.; Yamauchi, J.G.; Nemecz, Á.; Kim, C.; Ho, K.-Y.; Sharpless, K.B.; et al. Generation of Candidate Ligands for Nicotinic Acetylcholine Receptors via in situ Click Chemistry with a Soluble Acetylcholine Binding Protein Template. *Journal of the American Chemical Society* **2012**, *134*, 6732-6740, doi:10.1021/ja3001858.
44. Tieu, W.; Soares da Costa, T.P.; Yap, M.Y.; Keeling, K.L.; Wilce, M.C.J.; Wallace, J.C.; Booker, G.W.; Polyak, S.W.; Abell, A.D. Optimising in situ click chemistry: the screening and identification of biotin protein ligase inhibitors. *Chemical Science* **2013**, *4*, 3533-3537, doi:10.1039/C3SC51127H.
45. Camberlein, V.; Fléau, C.; Sierocki, P.; Li, L.; Gealageas, R.; Bosc, D.; Guillaume, V.; Warenghem, S.; Leroux, F.; Rosell, M.; et al. Discovery of the First Selective Nanomolar Inhibitors of ERAP2 by Kinetic Target-Guided Synthesis. *Angewandte Chemie (International ed. in English)* **2022**, *61*, e202203560, doi:10.1002/anie.202203560.

46. Parvatkar, P.T.; Wagner, A.; Manetsch, R. Biocompatible reactions: advances in kinetic target-guided synthesis. *Trends in Chemistry* **2023**, *5*, 657-671, doi:https://doi.org/10.1016/j.trechm.2023.06.002.
47. Millward, S.W.; Agnew, H.D.; Lai, B.; Lee, S.S.; Lim, J.; Nag, A.; Pitram, S.; Rohde, R.; Heath, J.R. In situ click chemistry: from small molecule discovery to synthetic antibodies. *Integrative Biology* **2013**, *5*, 87-95, doi:10.1039/c2ib20110k.
48. Oueis, E.; Sabot, C.; Renard, P.-Y. New insights into the kinetic target-guided synthesis of protein ligands. *Chemical Communications* **2015**, *51*, 12158-12169, doi:10.1039/C5CC04183J.
49. Manetsch, R.; Krasiński, A.; Radić, Z.; Raushel, J.; Taylor, P.; Sharpless, K.B.; Kolb, H.C. In Situ Click Chemistry: Enzyme Inhibitors Made to Their Own Specifications. *Journal of the American Chemical Society* **2004**, *126*, 12809-12818, doi:10.1021/ja046382g.
50. Krasiński, A.; Radić, Z.; Manetsch, R.; Raushel, J.; Taylor, P.; Sharpless, K.B.; Kolb, H.C. In Situ Selection of Lead Compounds by Click Chemistry: Target-Guided Optimization of Acetylcholinesterase Inhibitors. *Journal of the American Chemical Society* **2005**, *127*, 6686-6692, doi:10.1021/ja043031t.
51. Lewis, W.G.; Green, L.G.; Grynszpan, F.; Radić, Z.; Carlier, P.R.; Taylor, P.; Finn, M.G.; Sharpless, K.B. Click Chemistry In Situ: Acetylcholinesterase as a Reaction Vessel for the Selective Assembly of a Femtomolar Inhibitor from an Array of Building Blocks. *Angewandte Chemie International Edition* **2002**, *41*, 1053-1057, doi:https://doi.org/10.1002/1521-3773(20020315)41:6<1053::AID-ANIE1053>3.0.CO;2-4.
52. Unver, M.Y.; Gierse, R.M.; Ritchie, H.; Hirsch, A.K.H. Druggability Assessment of Targets Used in Kinetic Target-Guided Synthesis. *Journal of Medicinal Chemistry* **2018**, *61*, 9395-9409, doi:10.1021/acs.jmedchem.8b00266.
53. Gladysz, R.; Vrijdag, J.; Van Rompaey, D.; Lambeir, A.-M.; Augustyns, K.; De Winter, H.; Van der Veken, P. Efforts towards an On-Target Version of the Groebke–Blackburn–Bienaymé (GBB) Reaction for Discovery of Druglike Urokinase (uPA) Inhibitors. *Chemistry – A European Journal* **2019**, *25*, 12380-12393, doi:https://doi.org/10.1002/chem.201901917.
54. Morandi, S.; Morandi, F.; Caselli, E.; Shoichet, B.K.; Prati, F. Structure-based optimization of cephalothin-analogue boronic acids as β-lactamase inhibitors. *Bioorganic & Medicinal Chemistry* **2008**, *16*, 1195-1205, doi:https://doi.org/10.1016/j.bmc.2007.10.075.
55. Zhou, J.; Stapleton, P.; Haider, S.; Healy, J. Boronic acid inhibitors of the class A β-lactamase KPC-2. *Bioorganic & Medicinal Chemistry* **2018**, *26*, 2921-2927, doi:https://doi.org/10.1016/j.bmc.2018.04.055.
56. Zhou, J.; Stapleton, P.; Xavier-Junior, F.H.; Schatzlein, A.; Haider, S.; Healy, J.; Wells, G. Triazole-substituted phenylboronic acids as tunable lead inhibitors of KPC-2 antibiotic resistance. *European Journal of Medicinal Chemistry* **2022**, *240*, 114571, doi:https://doi.org/10.1016/j.ejmech.2022.114571.
57. Deprez-Poulain, R.; Hennuyer, N.; Bosc, D.; Liang, W.G.; Enée, E.; Marechal, X.; Charton, J.; Totobenazara, J.; Berte, G.; Jahklal, J.; et al. Catalytic site inhibition of insulin-degrading enzyme by a small molecule induces glucose intolerance in mice. *Nature Communications* **2015**, *6*, 8250, doi:10.1038/ncomms9250.
58. Kassu, M.; Parvatkar, P.T.; Milanes, J.; Monaghan, N.P.; Kim, C.; Dowgiallo, M.; Zhao, Y.; Asakawa, A.H.; Huang, L.; Wagner, A.; et al. Shotgun Kinetic Target-Guided Synthesis Approach Enables the Discovery of Small-Molecule Inhibitors against Pathogenic Free-Living Amoeba Glucokinases. *ACS Infectious Diseases* **2023**, *9*, 2190-2201, doi:10.1021/acsinfecdis.3c00284.
59. Nacheva, K.; Kulkarni, S.S.; Kassu, M.; Flanigan, D.; Monastyrskyi, A.; Iyamu, I.D.; Doi, K.; Barber, M.; Namelikonda, N.; Tipton, J.D.; et al. Going beyond Binary: Rapid Identification of Protein–Protein Interaction Modulators Using a Multifragment Kinetic Target-Guided Synthesis Approach. *Journal of Medicinal Chemistry* **2023**, *66*, 5196-5207, doi:10.1021/acs.jmedchem.3c00108.
60. Morandi, F.; Caselli, E.; Morandi, S.; Focia, P.J.; Blázquez, J.; Shoichet, B.K.; Prati, F. Nanomolar Inhibitors of AmpC β-Lactamase. *Journal of the American Chemical Society* **2003**, *125*, 685-695, doi:10.1021/ja0288338.
61. Krajnc, A.; Lang, P.A.; Panduwawala, T.D.; Brem, J.; Schofield, C.J. Will morphing boron-based inhibitors beat the β-lactamases? *Current Opinion in Chemical Biology* **2019**, *50*, 101-110, doi:https://doi.org/10.1016/j.cbpa.2019.03.001.
62. Sharpless, K.B.; Manetsch, R. In situ click chemistry: a powerful means for lead discovery. *Expert Opinion on Drug Discovery* **2006**, *1*, 525-538, doi:10.1517/17460441.1.6.525.

 doi:10.20944/preprints202503.0489.v1

63. Copeland, R.A. *Enzymes. A pratical Introduction to structure, mechanism and data analysis* second ed.; John Wiley & Sons: New York, 2000.
64. De Meester, F.; Joris, B.; Reckinger, G.; Bellefroid-Bourguignon, C.; Frère, J.-M.; Waley, S.G. Automated analysis of enzyme inactivation phenomena: Application to β-lactamases and DD-peptidases. *Biochemical Pharmacology* **1987**, *36*, 2393-2403, doi:https://doi.org/10.1016/0006-2952(87)90609-5.